The ancestral symbiont sensor kinase CSK links photosynthesis with gene expression in chloroplasts

Sujith Puthiyaveetil*, T. Anthony Kavanagh†, Peter Cain‡, James A. Sullivan*, Christine A. Newell§, John C. Gray§, Colin Robinson‡, Mark van der Giezen¶, Matthew B. Rogers¶, and John F. Allen*‖

*School of Biological and Chemical Sciences, Queen Mary, University of London, Mile End Road, London E1 4NS, United Kingdom; †Smurfit Institute of Genetics, Trinity College Dublin, Dublin 2, Ireland; ‡Department of Biological Sciences, University of Warwick, Coventry CV4 7AL, United Kingdom; §Department of Plant Sciences, University of Cambridge, Downing Street, Cambridge CB2 3EA, United Kingdom; and ¶Centre for Eukaryotic Evolutionary Microbiology, School of Biosciences, University of Exeter, Exeter EX4 4QD, United Kingdom

Communicated by Elisabeth Gantt, University of Maryland, College Park, MD, April 25, 2008 (received for review February 15, 2008)

We describe a novel, typically prokaryotic, sensor kinase in chloroplasts of green plants. The gene for this chloroplast sensor kinase (CSK) is found in cyanobacteria, prokaryotes from which chloroplasts evolved. The CSK gene has moved, during evolution, from the ancestral chloroplast to the nuclear genomes of eukaryotic algae and green plants. The CSK protein is now synthesised in the cytosol of photosynthetic eukaryotes and imported into their chloroplasts as a protein precursor. In the model higher plant *Arabidopsis thaliana*, CSK is autophosphorylated and required for control of transcription of chloroplast genes by the redox state of an electron carrier connecting photosystems I and II. CSK therefore provides a redox regulatory mechanism that couples photosynthesis to gene expression. This mechanism is inherited directly from the cyanobacterial ancestor of chloroplasts, is intrinsic to chloroplasts, and is targeted to chloroplast genes.

cell evolution | chloroplast genome | redox | transcription | two-component system

Photosynthesis is the conversion of radiant energy into chemical potential energy by land plants, algae, and certain species of bacteria. These organisms thereby harness sunlight to drive the biogeochemical cycles of carbon, nitrogen, and oxygen, fuelling and sustaining life on Earth. In eukaryotes, photosynthesis occurs in chloroplasts, cytoplasmic organelles that evolved from a free-living cyanobacterium. The ancient symbiosis that co-opted prokaryotic cyanobacteria as photosynthetic compartments of eukaryotic cells involved the uptake and maintenance of both the photosynthetic and genetic systems of the cyanobacterial endosymbiont. Today, the chloroplasts of photosynthetic eukaryotes carry out oxygenic photosynthesis that is indistinguishable, except in fine detail, from photosynthesis in cyanobacteria. In contrast, the chloroplast genome has been hugely decreased in size, because almost all cyanobacterial genes still retained by eukaryotes have relocated to the cell nucleus (1). Therefore the vast majority of chloroplast proteins are now imported as products of nuclear genes that encode chloroplast-targeted precursors made on cytosolic ribosomes (2).

The few functional genes now left in chloroplasts always include genes for core proteins of the photochemical reaction centers that perform the primary, light-driven redox chemistry of photosynthetic electron transfer (3). Expression of these chloroplast genes is regulated by photosynthetic electron transport (4). Here we demonstrate that the basis of regulation is a typically bacterial, two-component signaling system, inherited from the cyanobacterial ancestor of the chloroplast.

Two-component signal transduction is ubiquitous in prokaryotes (5), including cyanobacteria (6). Its components are a sensor kinase, phosphorylated on histidine when a specific environmental change occurs; and a response regulator that contains an aspartate residue to which the phosphate group is transferred, activating an appropriate response (5). The nuclear genome of the model higher plant *Arabidopsis thaliana* contains 54 genes for two-component proteins (7). However, known two-component elements in chloroplasts are limited to a few examples in certain nongreen algal groups, where there are just one or two two-component genes of uncertain function in the chloroplast genome itself (8).

Results and Discussion

Chloroplast Sensor Kinase (CSK) in *Arabidopsis thaliana*. We inspected the complete nuclear genome sequence of *Arabidopsis thaliana* for a sensor kinase that might be synthesised in the cytosol as a precursor for import into chloroplasts. Fig. 1 shows the deduced amino acid sequence of a predicted CSK, the *At1g67840* gene product of *Arabidopsis thaliana*, aligned with sequences of three bacterial histidine sensor kinases and of homologous proteins from whole genomes or expressed sequence tags (EST) of other plant and algal species. Fig. 1*A* shows the conserved histidine residue that is the site of autophosphorylation by phosphoryl group transfer from ATP. This histidine phosphorylation site is retained in CSKs of the red alga *Cyanidioschyzon merolae* and of the diatoms *Phaeodactylum tricornutum* and *Thalassiosira pseudonana* (Fig. 1*A*). In contrast, *Arabidopsis thaliana* CSK and other plant CSKs contain an homologous "H-box" motif in which the histidine phosphorylation site has been replaced by glutamic acid (Fig. 1*A*). In further contrast, the histidine phosphorylation site has been replaced by a tyrosine residue in the CSK of the eukaryotic alga *Ostreococcus* (9) (Fig. 1*A*). Similar replacement of the histidine residue of the original phosphorylation site has been observed in plant phytochromes (10) and ethylene receptors (11), which are serine/threonine kinases with histidine kinase ancestries. Fig. 1*B* shows the sequence motifs N, G1, F, G2, and G3 of the ATP-binding domain. It is seen that all of these motifs are common to the bacterial proteins ArcB (12), RegB (13), and EnvZ (14), and to the CSK proteins of *Arabidopsis thaliana*, *Populus trichocarpa*, *Oryza sativa*, *Thalassiosira pseudonana*, and *Cyanidioschyzon merolae* (Fig. 1*B*).

Subcellular Localization of CSK. The entire coding sequence of CSK (giving 611 aa) was fused in-frame with the gene for green fluorescent protein. Tobacco leaf epidermal cells were transformed with this full-length CSK-GFP gene construct. After 48 h, fluorescence microscopy revealed that the transiently expressed GFP was entirely colocated with chlorophyll fluorescence, showing that the CSK precursor is targeted and imported into chloroplasts (Fig. 2). A second CSK-GFP construct carrying only the first 139 aa residues

Author contributions: S.P. and J.F.A. designed research; S.P., T.A.K., P.C., C.A.N., and J.F.A. performed research; S.P., T.A.K., J.A.S., and M.v.d.G. contributed new reagents/analytic tools; S.P., T.A.K., P.C., J.C.G., C.R., M.v.d.G., M.B.R., and J.F.A. analyzed data; and S.P. and J.F.A. wrote the paper.

The authors declare no conflict of interest.

Freely available online through the PNAS open access option.

‖To whom correspondence should be addressed. E-mail: j.f.allen@qmul.ac.uk.

This article contains supporting information online at www.pnas.org/cgi/content/full/0803928105/DCSupplemental.

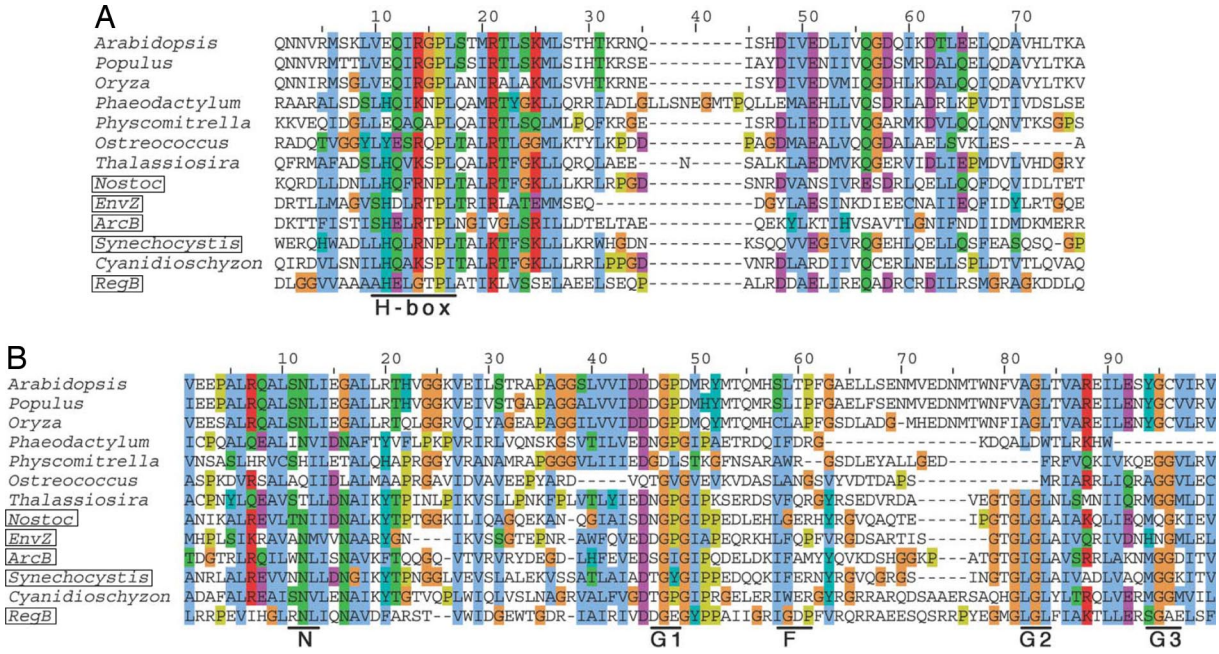

Fig. 1. Chloroplast sensor kinase (CSK) shows both conserved and divergent sequence features. Species names of prokaryotes are boxed. The colouring scheme of amino acids is based on their chemical properties and degree of conservation, and is the standard scheme of clustalx (36). (Red, basic; purple, acidic; blue, hydrophobic; green, polar and neutral; brown, glycine; khaki, proline; cyan, histidine and tyrosine). (*A*) CSK is a modified histidine kinase. The HisKA domain (dimerization and phosphoacceptor domain as defined by SMART database) of CSK aligns with those of its plant homologues and with those of three canonical histidine kinases, ArcB, RegB and EnvZ. The site of autophosphorylation, the H-box, is shown at the bottom. The autophosphorylating histidine is replaced by glutamate in CSK of land plants, whereas a tyrosine replaces this histidine in the CSK of *Ostreococcus*. The sequences shown for HisKA domains correspond to segments between and including the following amino acid positions of the full-length proteins. *A. thaliana*, 305–371; *P. patens*, 295–361; *O. lucimarinus*, 280- 40; *N. punctiforme*, 183–249; EnvZ (*E. coli*), 233–293; ArcB (*E. coli*), 282–347; *Synechocystis* sp PCC 6803, 175–240; *C. merolae*, 451–517; RegB (*R. capsulatus*), 195–261. For *P. deltoides*, *O. sativa*, *P. tricornutum* and *T. pseudonana*, the sequences are derived from ESTs and partial cDNAs. (*B*) The ATP-binding domain of CSK is conserved, as seen by sequence alignment of the ATP-binding domain of CSK and its homologues with that of ArcB, RegB and EnvZ from bacteria. The signature motifs (shown as N, G1, F, G2, and G3) characteristic of the ATP-binding domain of histidine kinases are largely conserved. The sequences shown for the ATP-binding domains correspond to segments between and including the following amino acid positions of the full-length proteins. *A. thaliana*, 478–602; *P. patens*, 472–584; O. *lucimarinus*, 435–534; *N. punctiforme*, 324–445; EnvZ (*E. coli*), 332–440; ArcB (*E. coli*), 394–507; *Synechocystis* sp PCC 6803, 308–432; *C. merolae*, 655–880; RegB (*R. capsulatus*), 303–423. For *P. trichocarpa*, *O. sativa*, *P. tricornutum* and *T. pseudonana*, the sequences are derived from ESTs and partial cDNAs.

of pre-CSK was also expressed in transformed tobacco epidermal cells became imported completely into chloroplasts (results not shown). To investigate further the location of CSK, a chloroplast import assay with the [^{35}S]methionine-labeled CSK precursor was executed *in vitro*. The radiolabeled CSK protein is seen to be imported into the major chloroplast soluble phase, the chloroplast stroma (Fig. 3*A*, lane S). Interestingly, the CSK transit peptide is not cleaved off, because the imported CSK has the same molecular mass as the initial translation product. Cleavage of the transit peptide after import is seen for the majority of chloroplast proteins, therefore a "low energy" binding assay (15) was carried out to ensure that CSK is a genuine chloroplast stromal protein. Under these low energy conditions—low temperature, without added ATP, and in darkness—chloroplasts bind protein precursors ready for import (15). This precursor binding is indeed seen in the case of CSK (Fig. 3*B*), where the precursor protein associates with chloroplasts (lane C), but remains sensitive to added protease. The function of the uncleaved transit peptide of CSK after import into the chloroplast (Figs. 2 and 3*A*) is unclear, but in the *Chlamydomonas* nuclear-encoded chlorophyll *a*/*b* binding protein, CP29, the

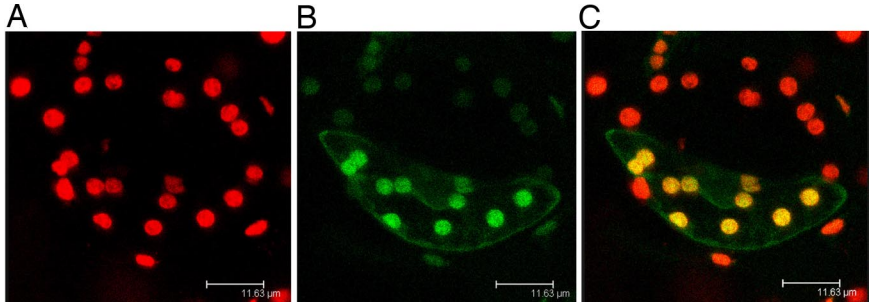

Fig. 2. The CSK precursor is synthesised in the cytosol and imported into chloroplasts. Leaves of *Nicotiana tabacum* (tobacco) were bombarded with tungsten particles coated with the pCSK2-GFP construct. After 48 h, confocal laser scanning microscopy revealed chlorophyll and GFP fluorescence. (*A*) Red fluorescence of chlorophyll identifies individual chloroplasts in a pair of stomatal guard cells. (*B*) Green fluorescence in one cell of the guard cell pair resulting from its transformation and expression of the CSK-GFP fusion protein. (*C*) Overlay of the images in *A* and *B* shows that the green fluorescence of the CSK-GFP fusion protein is localized in chloroplasts, where the combined fluorescence of chlorophyll and GFP appears orange.

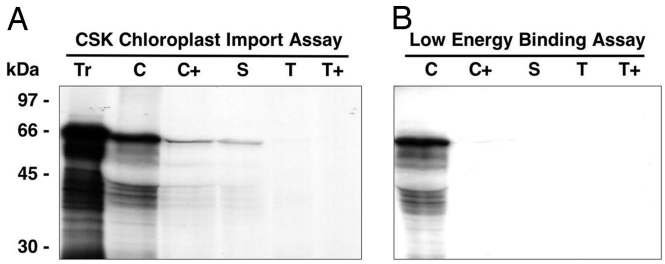

Fig. 3. The CSK is targeted into the chloroplast stroma. (*A*) The CSK is a stromal protein with an unprocessed transit peptide. A chloroplast import assay with the [^{35}S]methionine-labeled CSK precursor showed that the radiolabeled CSK protein is imported into the chloroplast stroma. The transit peptide is not cleaved off because the imported CSK has the same molecular mass as its precursor. (*B*) The CSK is a genuine chloroplast stromal protein. A 'low energy' binding assay showed that under low energy conditions, the radiolabeled CSK precursor binds to the chloroplast envelope, ready for import. The positions of molecular weight markers are indicated on the left. Tr, translation products; C, chloroplasts; C+, thermolysin digested chloroplasts; S, stroma; T, thylakoids; T+, trypsin digested thylakoids.

uncleaved transit peptide is a site of regulatory phosphorylation and acetylation (16).

CSK Links Photosynthetic Electron Transport with Chloroplast Transcription. Sensor kinases sense specific environmental cues and trigger appropriate responses via their cognate response regulator proteins. The latter are often DNA-binding transcription factors (5). We examined the transcriptional response of the chloroplast *psaA* gene to changes in light quality, and then compared the transcriptional response in wild-type *Arabidopsis thaliana* with that in two separate CSK T-DNA insertion lines from the Arabidopsis Biological Resource Center [supporting information (SI) Fig. S1]. It has been demonstrated in different plant species that transcription of the *psaA* gene, which encodes the photosystem I reaction center apoprotein A, responds robustly and in a functionally intelligible way to changes in the redox state of the electron carrier plastoquinone (4, 17, 18). Fig. 4 *A* and *B* shows the complex kinetics of *psaA* transcript accumulation in wild-type *Arabidopsis* plants. Here, Fig. 4 *A* and *B* also shows clear changes in these kinetics in the two *Arabidopsis* CSK-null mutants after shifts in the spectral quality of incident light that change the redox state of plastoquinone (18). The transcriptional response of CSK-mutant plants differs from that of wild-type plants. When light one (favoring photosystem I) is replaced by light two (favoring photosystem II), transcripts of the chloroplast *psaA* gene for the photosystem I reaction center protein PS I-A accumulate up to 11-fold in 26 h for the wild type (Fig. 4*A*). However, CSK-mutant plants show only a 5-fold increase in *psaA* gene transcription under the same conditions (Fig. 4*A*). The reverse light switch, from light two to light one, produces a 2.5-fold decrease in *psaA* expression in the wild type, as the reaction center of photosystem I is repressed (Fig. 4*B*). In contrast, *psaA* transcript quantity does not decrease under the same conditions in CSK mutants (Fig. 4*B*). Instead, the sign of the response is reversed, and *psaA* transcript quantity increases for 8 h, eventually falling between 26 and 32 h (Fig. 4*B*).

Normal *psaA* transcriptional control is part of an acclimatory response in chloroplasts called photosystem stoichiometry adjustment. The function of photosystem stoichiometry adjustment is to compensate for any deficiency in energy conversion at either photosystem I or photosystem II by increasing the quantity of the photosystem that will otherwise become rate-limiting to overall photosynthesis. The chlorophyll *a*/*b* ratio is a measure of the

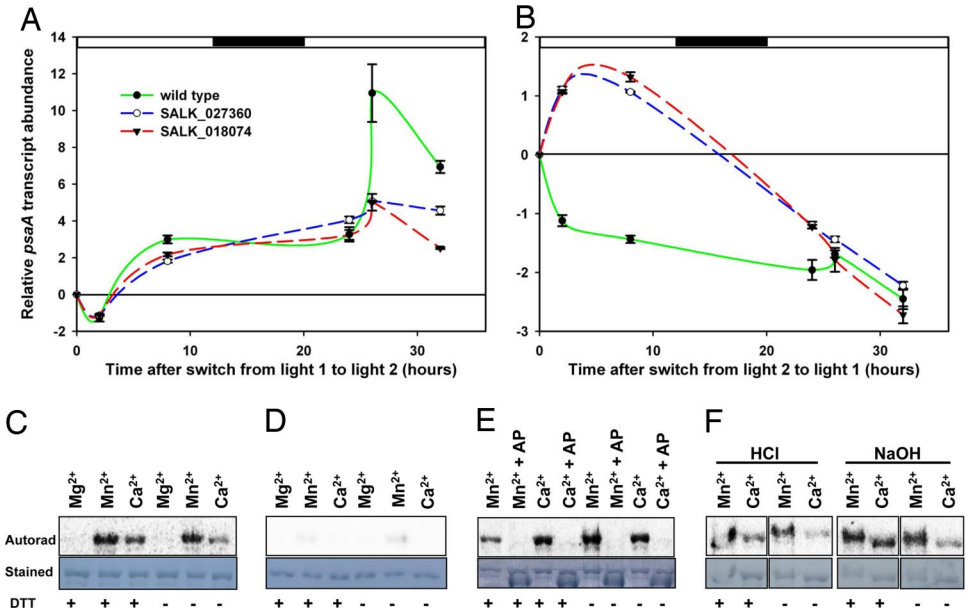

Fig. 4. Functional characterization of the *CSK*. (*A* and *B*) Inactivation of the *CSK* gene in *Arabidopsis* results in the loss of photosynthetic control of chloroplast gene transcription. The *psaA* gene transcription kinetics in wild-type and *CSK* knockout mutants, SALK_027360 and SALK_018074, as quantified with real time PCR. Changes in gene expression are shown as relative transcript abundance plotted against time. Experimental conditions are replacement of light one with light two and of light two with light one. The time point at which the lights are switched is taken as zero time and the fold change that follows (up- or down-regulation) is calculated by taking the expression at the time of light switch (zero time) as baseline. Error bars represent ± SE from three technical replicates. An eight-hour dark period is shown as the shaded rectangle on the *x* axis. (*C–F*) CSK is a phosphoprotein and appears to be its own protein kinase. Overexpressed and purified CSK-GST fusion protein becomes autophosphorylated in the presence of Mn^{2+} and Ca^{2+} (*C*). GST protein alone is not labeled sufficiently to account for the labeling of CSK-GST (*D*). Alkaline phosphatase treatment completely removes the labeling of the autophosphorylated CSK (*E*). Acid/base stability assay shows CSK phosphoryl group is resistant to both acid and alkali treatments (*F*). Autorad, the autoradiograph of the labeling reaction separated by SDS/PAGE; Stained, the amido black staining of the corresponding PVDF membrane from which the autoradiograph was developed. Divalent cation (Mg^{2+}/Mn^{2+}/Ca^{2+}) present in labeling reaction is shown above each lane. +AP above the divalent cation in *E* indicates treatment with alkaline phosphatase. The presence or absence of DTT, DTT, in the reaction medium is shown as + or − at the bottom of each lane.

Table 1. Chlorophyll *a*/*b* ratios in white light-grown, light 2-grown and light 1-grown wild-type and *CSK* mutant plants

Chl *a*/*b* ratio	Grown in white light	Grown under Light 2	Grown under Light 1
Wild type	2.27 ± 0.13	3.05 ± 0.03	1.55 ± 0.09
CSK mutant	2.32 ± 0.08	2.54 ± 0.05	2.10 ± 0.12

Data are shown as means ± SE from three independent measurements

stoichiometry of photosystem I to photosystem II (19). Table 1 shows the lack of a functional photosystem stoichiometry adjustment as an inability of the CSK mutants to control Chl *a*/*b* ratio in response to changes between light one and light two.

CSK Is Autophosphorylated. Autophosphorylation of sensor kinases is the initial step in the detection and transduction of signals by two-component signaling pathways. We therefore tested whether CSK becomes autophosphorylated by incubating the overexpressed CSK protein, which includes the catalytic domain of CSK fused with the GST tag, in the presence of [γ-^{32}P]ATP, the reducing agent DTT, and the divalent cations Mg^{2+}, Mn^{2+}, or Ca^{2+}. It is known that bacterial sensor kinases have specific requirements for certain divalent cations for autophosphorylation and signal perception. The CSK protein becomes autophosphorylated in the presence of Mn^{2+} and to a lesser degree in the presence of Ca^{2+}, but no autophosphorylation was detected in the presence of Mg^{2+} (Fig. 4*C*). DTT stimulates autophosphorylation but is not an absolute requirement (Fig. 4*C*). Manganese-specific autophosphorylation is known to be characteristic of some plant ethylene sensors that are derived from histidine sensor kinases (11, 20). Fig. 4*D* shows little or no labeling of the GST protein alone by [γ-^{32}P]ATP under any of these conditions. To further confirm that the labeling of CSK results from phosphorylation of an amino acid side chain by ^{32}P, the labeled proteins were incubated with calf intestine alkaline phosphatase, which hydrolyzes orthophosphoric acid monoester groups (21). Alkaline phosphatase treatment completely removed ^{32}P-labeling of CSK (Fig. 4*E*).

To investigate the identity of the phosphorylated amino acid(s) in autophosphorylated CSK, the autophosphorylated protein was incubated in acid or alkali. It is known that phosphohistidine is labile in acid but stable in alkaline solution, that phosphoserine and phosphothreonine are acid-stable and alkali-labile, and that phosphotyrosine is stable in both acid and alkali. The stability of the CSK phosphoryl group to both acid and alkali treatments (Fig. 4*F*) suggests tyrosine phosphorylation. Because a glutamate residue replaces the histidine autophosphorylation site in plant CSKs (Fig. 1*B*), conserved tyrosine residues lying outside the H- box could be the site(s) of phosphorylation of plant CSK. In CSK of the chlorophycean alga *Ostreococcus*, a tyrosine residue replaces histidine (Fig. 1*B*). Such a tyrosine replacement in the DivL sensor kinase of *Caulobacter crescentus* results in tyrosine autokinase activity of DivL (22).

Cyanobacterial Ancestry of CSK. Phylogenetic analysis of predicted CSK amino acid sequences from a red alga and a green alga and from two diatoms and five green plants shows that all CSKs share common ancestors with cyanobacterial histidine sensor kinases. In cyanobacteria, Hik2 is a conspicuous example of a CSK homologue (Fig. 5). Hik2 is a cognate sensor of the Rre1 response regulator (6). The gene for Rre1 (cyanobacterial nomenclature) is retained by red algal plastids as ycf29. CSK is therefore related to the two-component systems retained from cyanobacteria by red algal plastids. For example, in the single-celled ancient red alga *Cyanidioschyzon merolae*, CSK is a nuclear-encoded sensor kinase, and the only sensor kinase in the whole genome (23). The plastid of *C. merolae* encodes two response regulators, ycf29 and ycf27, both of

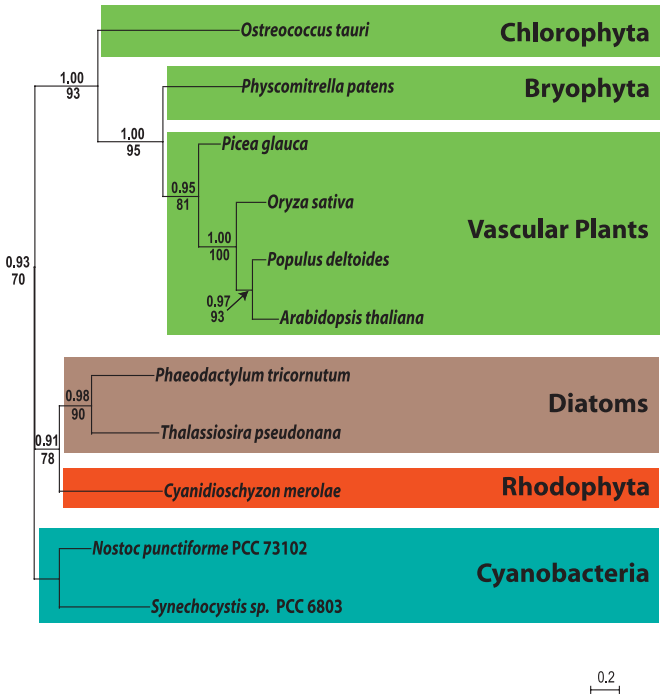

Fig. 5. CSK is present in all major plant and algal lineages and evolved from a Hik2-like cyanobacterial histidine sensor kinase. Bayesian phylogeny of Hik2, posterior probabilities are shown above nodes, PHYML 2.4.5. bootstrap values are shown below nodes.

which are transcription factors with a helix-turn-helix DNA binding motif (24). The cognate response regulator partner of CSK in higher plant chloroplasts remains to be identified.

Distribution and Function of CSK Suggest Deep Evolutionary Significance. The *CSK* gene homologue *Hik2* is retained as one of only four histidine sensor kinases in the minimal cyanobacterial genome of *Prochlorococcus marinus* SS120 (25). CSK is also retained in the minimal eukaryotic nuclear genomes of *Ostreococcus* (9) and *Cyanidioschyzon* (23). Furthermore, CSK has persisted through a secondary symbiotic event in the ancestor of diatoms such as *Phaeodactylum tricornutum* and *Thalassiosira pseudonana* where the chloroplast is derived from a eukaryotic, red algal symbiont, itself a product of a primary endosymbiosis involving a cyanobacterium. In green plants, CSK bears the unmistakable hallmarks of a cyanobacterial sensor kinase (Figs. 1 and 4 *C–F*) that is now targeted to chloroplasts (Figs. 2 and 3), being encoded by a gene that has moved, in evolution, from the chloroplast to the cell nucleus. The sequence (Fig. 1 and Figs. S2 and S3), functional (Fig. 4) and phylogenetic (Fig. 5) properties of CSK strongly suggest that CSK is the sensor in a two-component redox regulatory system that provides the mechanism that couples photosynthesis to chloroplast genome function. This coupling may also provide information controlling expression of nuclear genes for components of photosynthesis and gene expression in chloroplasts (17, 26).

Oxygenic photosynthesis takes place in chloroplasts and cyanobacteria, and requires two separate photochemical reaction centers that are connected electrically in series. Together with their distinct light-harvesting antennae, these reaction centers comprise photosystems I and II of the photosynthetic electron transport chain. CSK is clearly required for the photosynthetic, redox control of reaction center gene transcription (Fig. 4) that corrects imbalance in electron transport between the two photosystems by initiating new synthesis of proteins, according to the redox signal received from the connecting electron carrier, plastoquinone (4, 19).

Conclusion

Our results show that redox regulatory coupling is intrinsic to chloroplasts and has been inherited, and maintained, from the chloroplast's cyanobacterial ancestor. This coupling implies a general function for cytoplasmic genetic systems in eukaryotes. The persistence, in chloroplasts, of a bacterial two-component redox regulatory system is an explicit prediction of the CORR hypothesis for the function of chloroplast and mitochondrial genomes (3, 27). The CORR hypothesis (CO-location for Redox Regulation) states that genes have been retained in bioenergetic organelles to provide direct and unconditional regulation of their expression by the redox state of their gene products, the core proteins of energy transduction in photosynthesis and respiration. The properties and phylogenetic distribution of CSK are consistent with the application of CORR to chloroplasts, and in agreement with its predictions (3). Thus genes for photosynthetic reaction centers are retained in chloroplasts to be regulated by photosynthetic electron transport, whereas genes for the redox signaling components themselves belong to the major class of former cyanobacterial genes, and have moved to the cell nucleus.

Our findings support the hypothesis (3, 27) that local redox control of gene expression by energy transduction requires the presence of chloroplast and mitochondrial genomes as extranuclear genetic elements responsible for non-Mendelian inheritance of characters associated with photosynthesis and respiration.

Materials and Methods

Plant Growth Conditions. *Arabidopsis thaliana* seedlings were grown from seeds on soil at 24°C and a photon flux density of 100 μE m^{-2}·s^{-1} with an 8-hour light and 16-h dark photoperiod unless otherwise specified. For the Light switch time-course experiment, wild type (Col-0) and *CSK* knockout mutant *Arabidopsis* lines were grown in white light (100 μE m^{-2}·s^{-1}; 16-hour day) for 12 days and then transferred to light one or light two cabinets and allowed to acclimate for 4 days. At the end of the 4th day, light one was replaced by light two and vice versa. Leaves from 2 to 3 plants were collected for RNA extraction before the light switch and at various time points extending to 32 h after it. Chlorophyll *a*/*b* ratios were determined from plants that were 2–4 weeks old and grown under two days of light one, light two, or white light.

Lights One and Two. Light one was provided by two red fluorescent strip lamps (Osram L 18W/60 Red from Osram GmbH, Hellabrunner Strasse 1, 81536 Munich, Germany), each wrapped in red filter (Lee 027 medium red from Lee Filters, Andover, Hants, U.K.). Light two was provided by two white fluorescent strip lamps (Osram L 18W/827 Lumillux) each wrapped in orange filter (Lee 105 Orange). The photon flux density at the highest leaves in light two was 12 μE m^{-2}·s^{-1} and in light one was 6 μE m^{-2}·s^{-1}. Light one and light two were present for a 16-hour day (8-h dark period). The spectra of lights one and two show extended red and near infrared components in light one (results not shown). Their selective actions on photosystems I and II, respectively, were confirmed by modulated chlorophyll fluorescence and state transition measurements in the growth cabinet (results not shown).

Genotyping of the SALK T-DNA Insertion Lines. Two T-DNA lines (SALK_027360 and SALK_018074) harboring insertions in the gene (At1g67840) encoding the CSK protein were obtained from ABRC. Genomic DNA was isolated from these lines and genotyped for homozygous insertion lines by using genomic and T-DNA cassette primers. A reverse transcriptase PCR confirmed that expression from the locus At1g67840 was completely absent (see Fig. S1 and *SI Text* for details).

CSK-GFP Construct and Chloroplast Protein Import *in Vivo*. Two gene fusions between *Arabidopsis CSK* and the gene encoding the jellyfish green fluorescent protein (GFP) were constructed to investigate the subcellular targeting of CSK-GFP fusion proteins. The construct pCSK1-GFP was generated by amplifying a *CSK* cDNA fragment comprising 54 bp of the 5′UTR and the first 139 codons using Phusion DNA polymerase (New England Biolabs) and the oligonucleotide primers PK-F (5′-CTAggatccGAGAGTTTCAGTCTCAGCCACAAAGTAA-3′; lowercase sequence represents a BamH I cleavage site) and PK-R1 (5′-GTATaggcctCGAGAG-TACTGCGTTTGGATCAACGAT-3′; lowercase sequence represents a StuI cleavage site). The amplified cDNA was digested with BamH I and StuI and cloned in-frame with the GFP orf in the expression vector as described (28). The construct pCSK2-GFP contains a cDNA fragment possessing the same 5′ end but with the entire *CSK* ORF (without its stop codon) fused in-frame with GFP. This cDNA fragment was amplified by using the primer pair PK-F and PK-R2 (5′GTATaggcctTGCTTCATTG-GCTTCAGATACTGCTG).

Transcriptional control of the *CSK-GFP* gene fusions was provided by the cauliflower mosaic virus (CaMV) 35S promoter, and transcription termination and polyadenylation signals were provided by the nopaline synthase (*nos*) terminator (28). Leaves of *Nicotiana tabacum* (tobacco) were bombarded with tungsten particles (0.7 μm) coated with p*CSK*1-*GFP* or p*CSK*2-*GFP* by using a Bio-Rad PDS-1000/He particle delivery system, as described (29). After 24–48 h, leaf samples of 2 × 2 mm were mounted in water on a glass slide and viewed by scanning laser microscopy (TCS-NT, DMRXA light microscope stand, Leica Microsystems Wetzlar GmbH, Germany). Images of GFP and chlorophyll fluorescence, by using an excitation wavelength of 488 nm, were collected through TRITC and FITC filters, respectively.

Chloroplast Import of Radiolabeled CSK Precursor. Pea seedlings (*Pisum sativum*, var. Kelvedon Wonder) were grown and then harvested at 9 days old. Chloroplasts were isolated from the leaf tips as described (30). A full-length *CSK* cDNA clone was obtained from Genoscope (Paris) and the CSK precursor was synthesised by the method described in ref. 31 by using SP6 RNA-polymerase for cDNA transcription followed by translation in a wheat germ cell-free system in the presence of [^{35}S]methionine. Chloroplast import assays were conducted as before (32). Subsequent chloroplast fractionation and protease treatments are done as described before (33). Controls for chloroplast fractionation were based on published work (15). An identical import reaction was conducted omitting additional ATP, with the chloroplasts on ice, in the dark. These conditions promote envelope binding but inhibit import.

RNA Isolation and Quantitative Real Time PCR. Total RNA was isolated from the leaves of 15–17-day-old *Arabidopsis* plants with Qiagen RNeasy Plant mini kit. RNA was treated with RNase-free DNase (Qiagen) to eliminate possible DNA contamination. Real time quantitative RT PCR was performed with Quantitech SYBR green kit from Qiagen, in a Chromo4 cycler (Bio-Rad). A ≈150-bp-long sequence was amplified from the *psaA* and the reference gene, *Actin8* transcripts. For amplifying the *psaA* transcript, forward and reverse primers used were 5′ GGCACAAGCATCTCAGGTAA 3′ and 5′ AGCCCAAACAATGGATTCAA 3′ respectively and for *Actin8*, 5′ TTCCAGCAGATGTGGATCTCTA 3′ and 5′ AGAAAGAAAT-GTGATCCCGTCA 3′. The forward primer for the *Actin8* transcript was designed as flanking an intron-exon boundary, thus eliminating the chances of amplifying any contaminated DNA sequences. The optimum annealing temperature for the each primer pair was found out by a gradient PCR. The authenticities of the amplificates were confirmed by sequencing the PCR products. Amplification efficiency for each primer pair was calculated by a 16-fold serial dilution of the template and the R^2 value for each primer pair was found to be ≥0.99. A nontemplate control reaction was done for each primer pair to check whether template contamination or primer dimers contribute to the fluorescence signals observed. A small fluorescence signal at very late cycle numbers was seen in nontemplate control reactions for some primer pairs. This signal is likely to have arisen from primer dimers. A non-RT (non-reverse transcriptase) control reaction was also included to check for amplification from any contaminated DNA and it was found that, like nontemplate controls, a small fluorescence signal appeared at very late cycle numbers. For measuring the transcription kinetics of light switch samples, RNA was pooled from 2 to 3 plants and 3 technical replicates were used for each reaction. Expression values were normalized to total RNA. The quantitative real-time PCR technique used here employs relative quantification based on comparative C_T method.

Chlorophyll Estimation. Chlorophyll content was estimated by methods established by Porra *et al.* as described in ref. 19.

Autophosphorylation Assay. A partial cDNA clone (U13211) encoding 450 residues from the carboxy-terminus of CSK, which includes the catalytic domain was obtained from ABRC. The cDNA was cloned into pGEX4T2 (Amersham) vector system and expressed as a GST fusion protein. The over-expressed CSK-GST fusion protein was purified by affinity chromatography (glutathione sepharose). For autophosphorylation assay, ≈10 μg of CSK-GST protein was taken in a 25-μl reaction volume containing 50 mM Tris, pH 7.5, 50 mM KCl, 10% glycerol, 0.5 mM ATP, 8μCi [γ-^{32}P]ATP (3,000 Ci/mmol), with or without 2 mM DTT and 10 mM $MgCl_2$ or $MnCl_2$, or $CaCl_2$. The reactions were incubated at 22°C for 60 min and terminated by adding sample buffer. The phosphorylated proteins were subjected to SDS-12% PAGE and blotted onto PVDF membrane (Hybond-P, Amersham). The incorporated phosphate was visualized by autoradiography. The identity of the autophosphorylated CSK-GST fusion protein was confirmed by a monoclonal antibody directed against the GST tag (Novagen) of the fusion protein (results not shown). Standard Western blot analysis procedures

were followed for the immunodetection of the GST tag. Amido black staining of the same membrane was also performed to verify the protein loading. For dephosphorylation of the phosphorylated CSK protein, autophosphorylation of CSK protein was performed as above and 1 μl of calf intestine alkaline phosphatase (New England Biolabs) was added to the autophosphorylated CSK and incubated at 37°C for 30 min. Acid/alkali stability of the incorporated phosphate was determined by incubating the membrane in 1 M HCl or 3 M NaOH for 2 h at room temperature. The acid/alkali treated membrane was then rinsed with water and subjected to autoradiography.

Sequence Analysis. Sequence similarity searches were performed with blastp and tblastn programs. Subcellular localization prediction was carried out with the programs TargetP, ChloroP, WoLF PSORT, PCLR and Predotar. Domains and motifs were identified by using the SMART database. Sequence alignment was generated with ClustalW and the alignment was edited with Jalview.

Phylogenetic Reconstruction. Multiple alignment of the amino acid sequence corresponding to the catalytic domain of CSK and its homologues (as delineated by SMART database) was generated across a representative selection of photosynthetic eukaryotes and cyanobacteria. Sequences were retrieved from both JGI and GENBANK databases. The multiple alignment was generated by using CLUSTAL X and adjusted manually by using MacClade 4.06. The CSK tree was reconstructed from 91 characters. Bayesian phylogeny was generated by using Mr. Bayes 3.1 (34) from 2,000,000 generations divided between two parallel runs of 1,000,000 each with sampling every 1,000 generations. Although the likelihoods for both trees rapidly reached a plateau, 100 burn-in trees were nevertheless removed from both runs when computing the Bayesian topology. The substitution model was inferred by using a mixed model of amino acid substitution and rate across sites variation was modeled on a discrete gamma distribution approximated by using 4 gamma categories and 1 category of invariable sites. Bootstraps were generated by using PHYML 2.4.5 (35) using the WAG substitution model and rate-across-sites variation modeled on an approximate gamma distribution also using four gamma categories and one category of invariable sites.

ACKNOWLEDGMENTS. We thank Thomas Pfannschmidt and Carol A. Allen for discussions. S.P. thanks Queen Mary, University of London for a postgraduate research studentship; J.F.A. thanks The Royal Society of London for a Royal Society-Wolfson Research Merit Award; and M.B.R. is supported by a Wellcome Trust research grant to M.v.d.G.

1. Martin W, *et al.* (2002) Evolutionary analysis of Arabidopsis, cyanobacterial, and chloroplast genomes reveals plastid phylogeny and thousands of cyanobacterial genes in the nucleus. *Proc Natl Acad Sci USA* 99:12246–12251.
2. Ellis RJ (1984) The nuclear domination of chloroplast development. *Sci Prog Oxf* 69:129–142.
3. Allen JF (2003) The function of genomes in bioenergetic organelles. *Philos Trans R Soc Lond Ser B-Biol Sci* 358:19–37.
4. Pfannschmidt T, Nilsson A, Allen JF (1999) Photosynthetic control of chloroplast gene expression. *Nature* 397:625–628.
5. Stock AM, Robinson VL, Goudreau PN (2000) Two-component signal transduction. *Annu Rev Biochem* 69:183–215.
6. Ashby MK, Houmard J (2006) Cyanobacterial two-component proteins: structure, diversity, distribution, and evolution. *Microbiol Mol Biol Rev* 70:472–509.
7. Hwang, I, Chen HC, Sheen J (2002) Two-component signal transduction pathways in Arabidopsis. *Plant Physiol* 129:500–515.
8. Duplessis MR, *et al.* (2007) Chloroplast His-to-Asp signal transduction: a potential mechanism for plastid gene regulation in Heterosigma akashiwo (Raphidophyceae). *BMC Evol Biol* 7:70.
9. Derelle E, *et al.* (2006) Genome analysis of the smallest free-living eukaryote Ostreococcus tauri unveils many unique features. *Proc Natl Acad Sci USA* 103:11647–11652.
10. Yeh KC, Lagarias JC (1998) Eukaryotic phytochromes: Light-regulated serine/threonine protein kinases with histidine kinase ancestry. *Proc Natl Acad Sci USA* 95:13976–13981.
11. Moussatche P, Klee HJ (2004) Autophosphorylation activity of the Arabidopsis ethylene receptor multigene family. *J Biol Chem* 279:48734–48741.
12. Iuchi S, Lin ECC (1992) Mutational analysis of signal transduction by ArcB, a membrane sensor protein responsible for anaerobic repression of operons involved in the central aerobic pathways in *Escherichia coli*. *J Bacteriol* 174:3972–3980.
13. Bauer C, Elsen S, Swem LR, Swem DL, Masuda S (2003) Redox and light regulation of gene expression in photosynthetic prokaryotes. *Philos Trans R Soc Lond Ser B-Biol Sci* 358:147–153; discussion 153–4.
14. Mizuno T, Wurtzel ET, Inouye M (1982) Osmoregulation of gene expression. II. DNA sequence of the *envZ* gene of the *ompB* operon of *Escherichia coli* and characterization of its gene product. *J Biol Chem* 257:13692–13698.
15. Friedman AL, Keegstra K (1989) Chloroplast protein import: Quantitative analysis of precursor binding. *Plant Physiol* 89:993–999.
16. Turkina MV, Villarejo A, Vener AV (2004) The transit peptide of CP29 thylakoid protein in *Chlamydomonas reinhardtii* is not removed but undergoes acetylation and phosphorylation. *FEBS Lett* 564:104–108.
17. Fey V, *et al*. (2005) Retrograde plastid redox signals in the expression of nuclear genes for chloroplast proteins of *Arabidopsis thaliana*. *J Biol Chem* 280:5318–5328.
18. Puthiyaveetil S, Allen JF (2008) Transients in chloroplast gene transcription. *Biochem Biophys Res Commun* 368:871–874.
19. Pfannschmidt T, Nilsson A, Tullberg A, Link G, Allen JF (1999) Direct transcriptional control of the chloroplast genes *psbA* and *psaAB* adjusts photosynthesis to light energy distribution in plants. *IUBMB Life* 48:271–276.
20. Zhang ZG, *et al.* (2004) Evidence for serine/threonine and histidine kinase activity in the tobacco ethylene receptor protein NTHK2. *Plant Physiol* 136:2971–2981.
21. Coleman JE (1992) Structure and mechanism of alkaline phosphatase. *Annu Rev Biophys Biomol Struct* 21:441–483.
22. Wu J, Ohta N, Zhao JL, Newton A (1999) A novel bacterial tyrosine kinase essential for cell division and differentiation. *Proc Natl Acad Sci USA* 96:13068–13073.
23. Matsuzaki M, *et al.*(2004) Genome sequence of the ultrasmall unicellular red alga *Cyanidioschyzon merolae* 10D. *Nature* 428:653–657.
24. Martinez-Hackert E, Stock AM (1997) Structural relationships in the OmpR family of winged-helix transcription factors. *J Mol Biol* 269:301–312.
25. Dufresne A, *et al.* (2003) Genome sequence of the cyanobacterium *Prochlorococcus marinus* SS120, a nearly minimal oxyphototrophic genome. *Proc Natl Acad Sci USA* 100:10020–10025.
26. Koussevitzky S, *et al.* (2007) Signals from chloroplasts converge to regulate nuclear gene expression. *Science* 316:715–719.
27. Allen JF (1993) Control of gene-expression by redox potential and the requirement for chloroplast and mitochondrial genomes. *J Theor Biol* 165:609–631.
28. Helliwell CA, *et al.* (2001) A plastid envelope location of *Arabidopsis ent*-kaurene oxidase links the plastid and endoplasmic reticulum steps of the gibberellin biosynthesis pathway. *Plant J* 28:201–208.
29. Hibberd JM, Linley PJ, Khan MS, Gray JC (1998) Transient expression of green fluorescent protein in various plastid types following microprojectile bombardment. *Plant J* 16:627–632.
30. Brock IW, *et al.* (1993) Precursors of one integral and five lumenal thylakoid proteins are imported by isolated pea and barley thylakoids: Optimisation of *in vitro* assays. *Plant Mol Biol* 23:717–725.
31. James HE, *et al.* (1989) Transport of proteins into chloroplasts. Import and maturation of precursors to the 33-Kda, 23-Kda, and 16-Kda proteins of the photosynthetic oxygen-evolving complex. *J Biol Chem* 264:19573–19576.
32. Mould RM, Robinson C (1991) A proton gradient is required for the transport of two lumenal oxygen-evolving proteins across the thylakoid membrane. *J Biol Chem* 266:12189–12193.
33. Di Cola A, Robinson C (2005) Large-scale translocation reversal within the thylakoid Tat system *in vivo*. *J Cell Biol* 171:281–289.
34. Ronquist F, Huelsenbeck JP (2003) MrBayes 3: Bayesian phylogenetic inference under mixed models. *Bioinformatics* 19:1572–1574.
35. Guindon S, Gascuel O (2003) A simple, fast, and accurate algorithm to estimate large phylogenies by maximum likelihood. *Syst Biol* 52:696–704.
36. Chenna R, *et al.* (2003) Multiple sequence alignment with the Clustal series of programs. *Nucleic Acids Res* 31:3497–3500.

Supporting information

Puthiyaveetil *et al.* 10.1073/pnas.0803928105

SI Text

Genotyping of SALK T-DNA Lines. The phenotypes identified and described for chloroplast sensor kinase (CSK) are based on two completely characterized T-DNA lines, SALK_027360 and SALK_018074, which harbor insertions in the At1g67840 locus encoding the CSK protein. Seeds for SALK_027360 and SALK_018074 lines were obtained from the European Arabidopsis Stock Center (Nottingham), sown on soil and the F_1 plants were selfed. A PCR based approach was used to identify homozygous insertion lines among the F_1 plants. Seeds obtained from the genotyped, F_1 homozygous plants were used to characterize the phenotype. The PCR based genotyping approach involved a genomic PCR using genomic primers, a second PCR using genomic and T-DNA left border primers and a third reverse transcriptase PCR (RT-PCR) to confirm the absence of transcripts from the At1g67840 locus. The positions of the T-DNA insertion in SALK_027360 and SALK_018074 lines are indicated in supporting information (SI) Fig. S1. Fig. S1*B* shows results from a genomic PCR using 5′ TGGCCTCTTTTAGCTATGGGGA 3′ as the forward primer and 5′ TGCTCAAGACAAAGCCGTTGA 3′ as the reverse primer. The wild type *CSK* gene was amplified from the wild type sample and not from the SALK_027360 sample indicating T-DNA insertion. Fig. S1*C* shows results from a genomic PCR using 5′ TGGCCTCTTTTAGCTATGGGGA 3′ as forward primer and 5′ GCGTGGACCGCTTGCTGCAACT 3′ as reverse primer, which is also the T-DNA cassette left border primer. The length of the amplicon from this second PCR is indicative of the approximate insertion site in the SALK_027360. The actual insertion site was further determined by sequencing the amplificate from this PCR. Fig. S1*D* shows results from a reverse transcriptase PCR using 5′ GAGAGTTTCAGTCTCAGCCACA 3′ as forward primer and 5′ TTGCAATCAATTTTGTTCAAGTC 3′as reverse primer. The *CSK* mRNA was amplified only from the wild type and not from the SALK_027360 line, thus confirming that the At1g67840 locus was not transcribed in the SALK_027360 line. Fig. S1*E* shows results from a genomic PCR using 5′ GTAGAGTTCACACAGATGATTGAGAAA 3′ as the forward primer and 5′ GCTTCATTGGCTTCAGATACTGC 3′ as the reverse primer. The wild type *CSK* gene is amplified from the wild type sample and not from the SALK_018074 sample, indicating T-DNA insertion. Fig. S1*F* shows results from a genomic PCR using 5′ GCGTGGACCGCTTGCTGCAACT 3′ as the forward primer, which is also the T-DNA cassette left border primer, and 5′ GCTTCATTGGCTTCAGATACTGC 3′ as the reverse primer. The length of the amplificate from this PCR is indicative of the approximate insertion site in the SALK_018074. The actual insertion site was further determined by sequencing the amplificate from this PCR. Fig. S1*G* shows results from a reverse transcriptase PCR using 5′ ATGCTTCTTTCTGCAATCGC 3′ as the forward primer and 5′ CTATGCTTCATTGGCTTCAG 3′as the reverse primer. The *CSK* mRNA was amplified only from the wild type and not from the SALK_018074 line, thus confirming that the At1g67840 locus is not transcribed in the SALK_018074 line.

Conserved Sequence Features of the Chloroplast Sensor Kinase (CSK). Sequence prediction based on SMART, Pfam and InterPro database searches showed conserved functional domains in CSK (Fig. S3). These include an ATP-binding domain (HATPase_c) toward the C terminus, and a domain characteristic of a site of histidine autophosphorylation site and dimerisation (HisKA), consistent with a function for CSK as a sensor kinase. It should be mentioned that the HisKA domain in CSKs of *A. thaliana*, *P. patens* and *O. lucimarinus*, although recognizable in SMART, Pfam, and InterPro databases, is not predicted by the secondary database Prosite. N-terminal to the HisKA domain is a GAF domain, which presumably forms the redox sensor input domain of CSKs. GAF domain and the related PAS redox sensor input domain are known to sense redox signals via redox-active prosthetic groups such as heme (1) or flavin adenine dinucleotide (FAD) (2). The Prosite database predicts a nucleotide-binding motif in the GAF domain of the *Arabidopsis* CSK. This observation is consistent with the nucleotide binding properties of some GAF domains (3) and raises the interesting possibility that the GAF domain in CSK binds one or more redox-responsive cofactors such as uridine or flavin nucleotides for its redox-sensing function. Some redox sensor kinases are also known to employ redox-responsive cysteine residues, residing within the PAS/GAF domains (4, 5) or seen as part of other separate redox sensor input domains (6) for sensing redox signals. A conserved cysteine residue is seen within the GAF domain of plant and cyanobacterial CSKs (Fig. S2). While GAF domains of CSKs in *Ostreococcus*, *Phaeodactylum*, and a few *Synechococcus* species do not seem to have this cysteine conserved (Fig. S2), other positionally conserved cysteines are present in their GAF domains (Fig. S2).

Conserved Functional Domains in CSK. Fig. S3 shows conserved functional domains in CSK and representative algal and cyanobacterial homologues (redrawn from SMART database predictions). Domain denotations: HATPase_c, ATP-binding domain; HisKA, site of histidine autophosphorylation and dimerisation; GAF, sensor domain. For the *Ostreococcus* and the *Physcomitrella* CSKs, the predicted GAF domain is below the curated threshold score of SMART database. For the *Arabidopsis* CSK, SMART database does not predict a GAF domain, even though the *Arabidopsis* CSK sensor domain shows significant sequence homology to the GAF domain of cyanobacterial Hik2. Domain boundary of GAF domains, which fall below the curated threshold score, or not predicted by SMART database, are shown in broken lines. The chloroplast-targeting signal is represented as a white rectangle at the N terminus.

Sequence Features of CSK Suggest Mechanisms of Redox Sensing. Further sequence prediction based on SMART database searches shows a conserved GAF domain in cyanobacterial CSK homologues and in algal and plant CSKs (Fig. S2 and Fig. S3). A GAF domain is a small ligand-binding domain first described for vertebrate c*G*MP specific phosphodiesterase, a cyanobacterial *A*denylate cyclase and the bacterial formate hydrogen lyase transcription activator *F*hlA. GAF domains are known to form sensor domains in a number of histidine kinases. GAF domains of redox histidine sensor kinases sense redox signals via a redox-active heme prosthetic group (7) or by a conserved redox-responsive cysteine residue (5). GAF domains also show homology and functional overlap with the well characterized redox sensor input domain, PAS (1, 8). A redox sensing and transcriptional regulatory role for CSK in chloroplasts is strongly suggested by its redox sensing sequence features (Fig. S2 and Fig. S3); by the observed signaling phenotypic effect of CSK (Fig. 4); and by the functional and phylogenetic relatedness of CSK to the known transcriptional regulatory two-component systems of non-green algae. Our proposed redox-sensing role for CSK is

further supported by the demonstration that the cyanobacterial homologue of CSK, Hik2, interacts with the known redox response regulator, RppA (9) and confers tolerance of photosystem II to environmental stress (10). The cognate response regulator partner of CSK in higher plant chloroplasts remains to be elucidated. However, we can conclude that, like CSK itself, any chloroplast response regulator (CRR) is now nuclear encoded and imported into chloroplasts as a protein precursor. A modified response regulator-like protein, TCP34 is imported as the product of nuclear gene and specifically binds promoters of reaction center genes in spinach chloroplasts (11).

1. Sardiwal S, *et al.* (2005) GAF domain in the hypoxia/NO-inducible *Mycobacterium tuberculosis* DosS protein binds haem. *J Mol Biol* 353:929–936.
2. Taylor BL (2007) Aer on the inside looking out: Paradigm for a PAS-HAMP role in sensing oxygen, redox and energy. *Mol Microbiol* 65:1415–1424.
3. Zoraghi R, Corbin JD, Francis SH (2004) Properties and functions of GAF domains in cyclic nucleotide phosphodiesterases and other proteins. *Mol Pharmacol* 65:267–278.
4. Malpica R, Franco B, Rodriguez C, Kwon O, Georgellis D (2004) Identification of a quinone-sensitive redox switch in the ArcB sensor kinase. *Proc Natl Acad Sci USA* 101:13318–13323.
5. Vuillet L, *et al.*(2007) Evolution of a bacteriophytochrome from light to redox sensor. *EMBO J* 26:3322–3331.
6. Swem LR, *et al.* (2003) Signal transduction by the global regulator RegB is mediated by a redox-active cysteine. *EMBO J* 22:4699–4708.
7. Kumar A, Toledo JC, Patel RP, Lancaster JR, Jr, Steyn AJ (2007) *Mycobacterium tuberculosis* DosS is a redox sensor and DosT is a hypoxia sensor. *Proc Natl Acad Sci USA* 104, 11568–11573.
8. Ho YS, Burden LM, Hurley JH (2000) Structure of the GAF domain, a ubiquitous signaling motif and a new class of cyclic GMP receptor. *EMBO J* 19:5288–5299.
9. Sato S, *et al.* (2007) A large-scale protein protein interaction analysis in *Synechocystis* sp. PCC6803. *DNA Res* 14:207–216.
10. Mikami K, *et al.* (2003) Histidine kinases, Hik2, Hik16 and Hik33, in *Synechocystis* sp. PCC 6803 are involved in the tolerance of photosystem II to environmental stress. *Plant Cell Physiol* 44:S82.
11. Weber P, *et al.* (2006) TCP34, a nuclear-encoded response regulator-like TPR protein of higher plant chloroplasts. *J Mol Biol* 357:535–549.

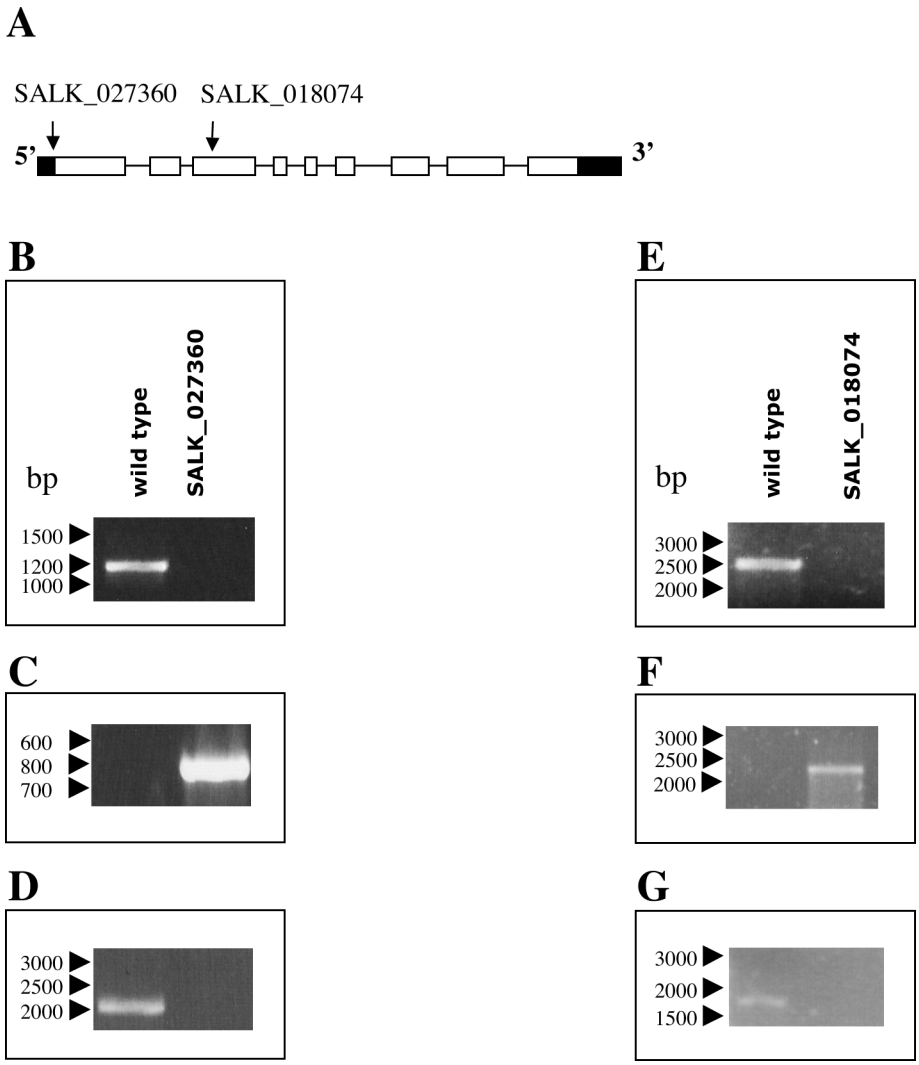

Fig. S1. (*A*) Schematic representation of the gene region of CSK indicating T-DNA insertion sites in two different SALK lines. Exons are represented as white rectangles and introns as the lines connecting them. The UTR regions at either end of the transcript are shown as filled rectangles. (*B–G*) Results from the genomic and the reverse transcriptase PCR methods used for genotyping SALK_027360 and SALK_018074 lines.

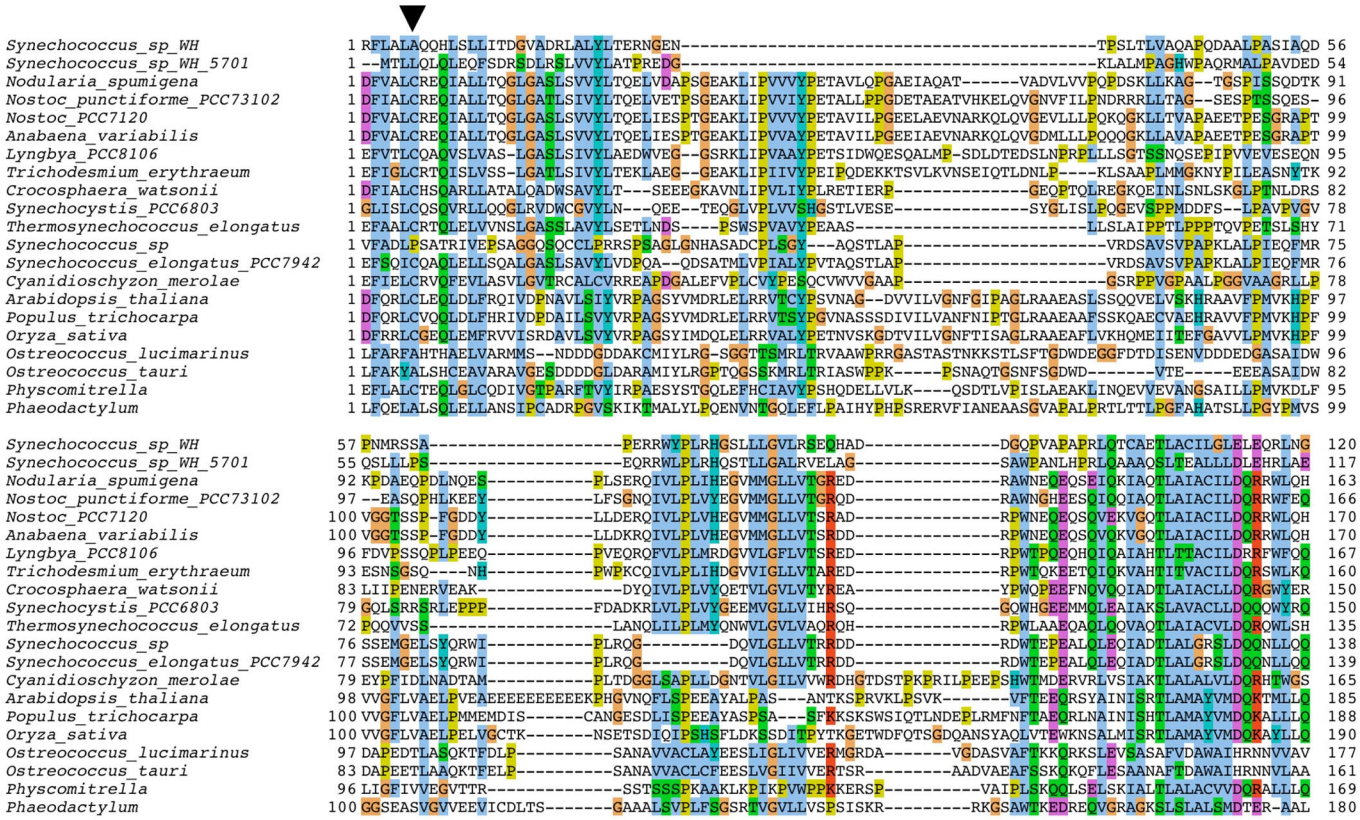

Fig. S2. Sequence alignment of the predicted GAF domain of the *Arabidopsis thaliana* CSK and its plant, algal, and cyanobacterial homologues (as delineated and named by the SMART database). The conserved cysteine residue in the cyanobacterial and plant CSKs is indicated by the arrowhead.

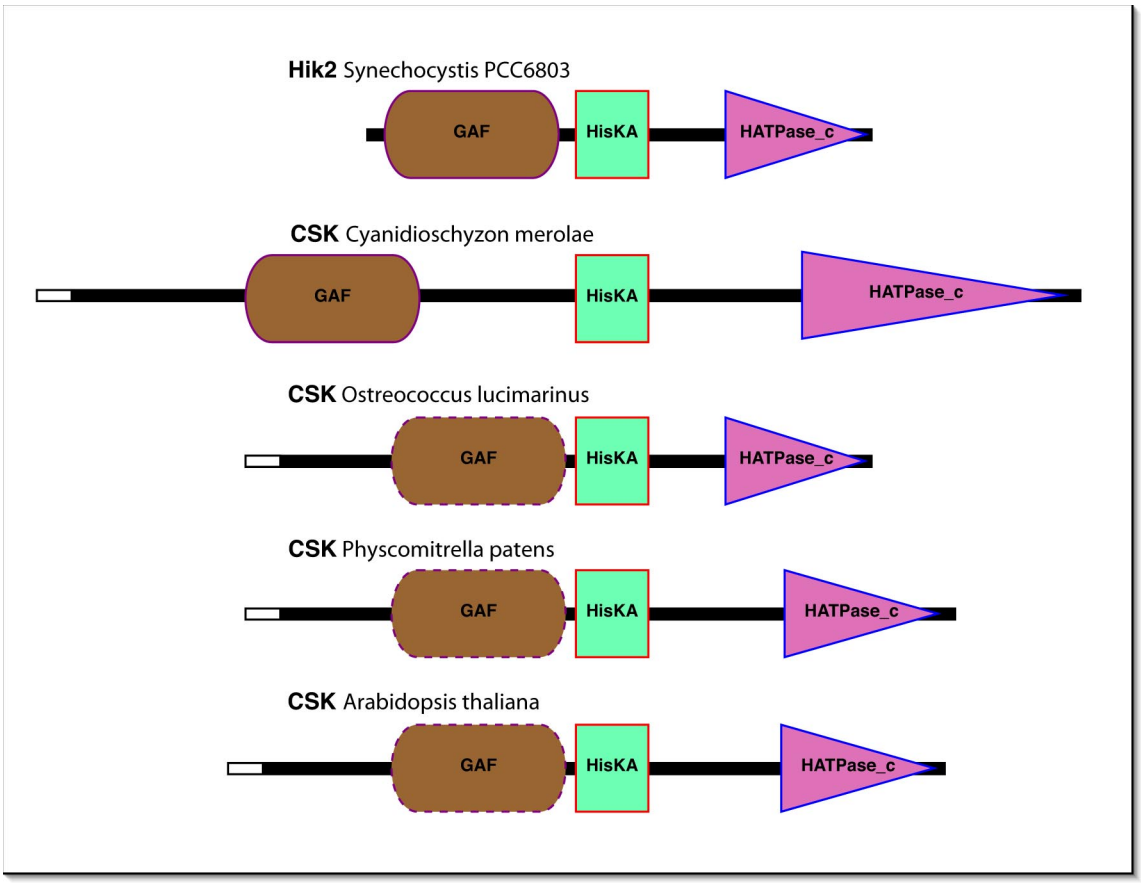

Fig. S3. Conserved functional domains in CSK and representative algal and cyanobacterial homologues (redrawn from SMART database predictions). For the *Ostreococcus* and the *Physcomitrella* CSKs, the predicted GAF domain is below the curated threshold score of SMART database. For the *Arabidopsis* CSK, SMART database does not predict a GAF domain, even though the *Arabidopsis* CSK sensor domain shows significant sequence homology to the GAF domain of cyanobacterial Hik2. Domain boundaries of GAF domains which fall below the curated threshold score or which are not predicted by SMART database are shown in broken lines. The chloroplast targeting signal is depicted as a white rectangle at the N terminus. Domain denotations: HATPase_c, ATP-binding domain; HisKA, site of histidine auto phosphorylation and dimerisation; GAF, sensor domain.